

Supporting Information for Activating MoS₂ basal planes for hydrogen evolution through direct CVD morphology controlling

Lianqing Dong [†], Shaoqiang Guo [†], Yuyan Wang [†], Qinghua Zhang [‡], Lin Gu [‡],
Caofeng Pan [§], Junying Zhang ^{†*}

[†] Key laboratory of Micro-nano Measurement, Manipulation and Physics (Ministry of Education), Department of Physics, Beihang University, Beijing 100191, China

[‡] Beijing National Laboratory for Condensed Matter Physics Institute of Physics, Chinese Academy of Sciences, Beijing 100190, China

[§] Beijing Institute of Nanoenergy and Nanosystems, Chinese Academy of Sciences, Beijing 100083, China

*Corresponding Author: zjy@buaa.edu.cn (J. Y. Zhang)

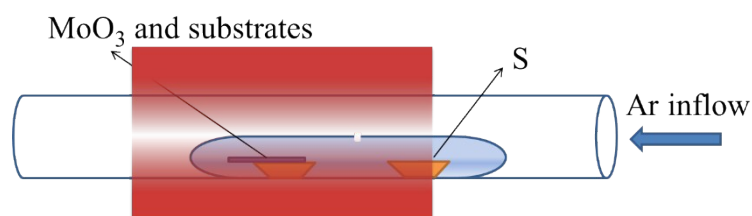


Fig. S1 Schematic illustration of the CVD system.

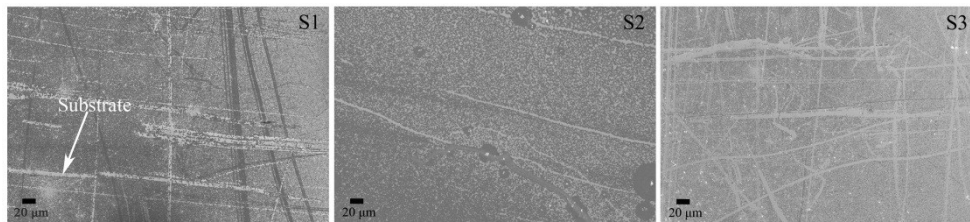


Fig. S2 The same coverage of different samples with hexagonal monolayer MoS₂ flakes.

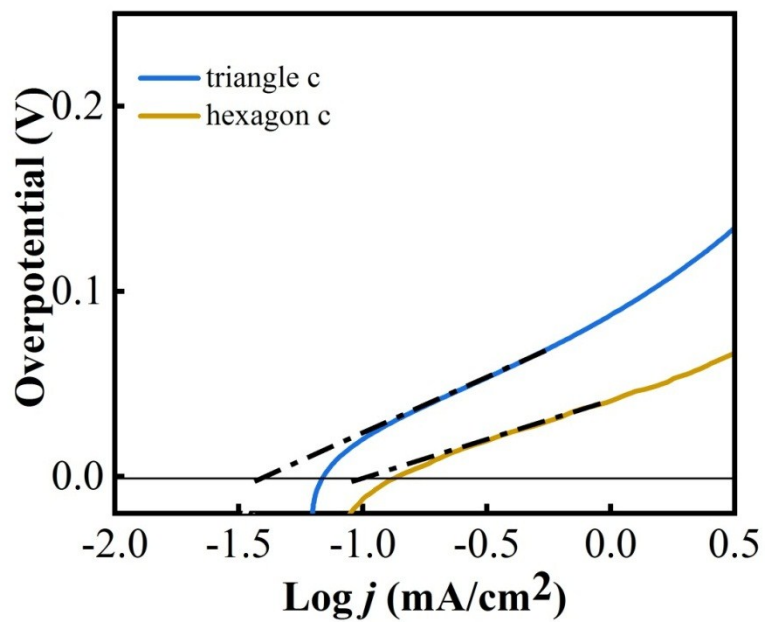


Fig. S3 Calculated exchange current densities of triangle and hexagon samples by applying an extrapolation method to the Tafel plots.

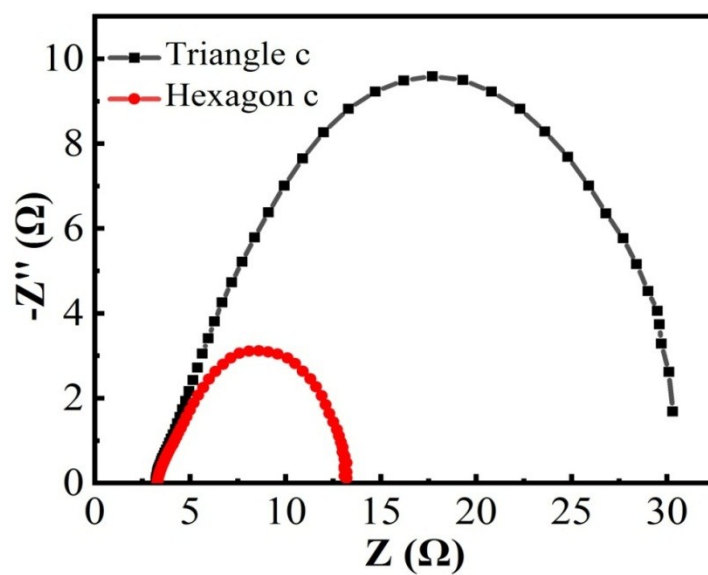


Fig. S4 Nyquist curves of Triangle c and Hexagon c.

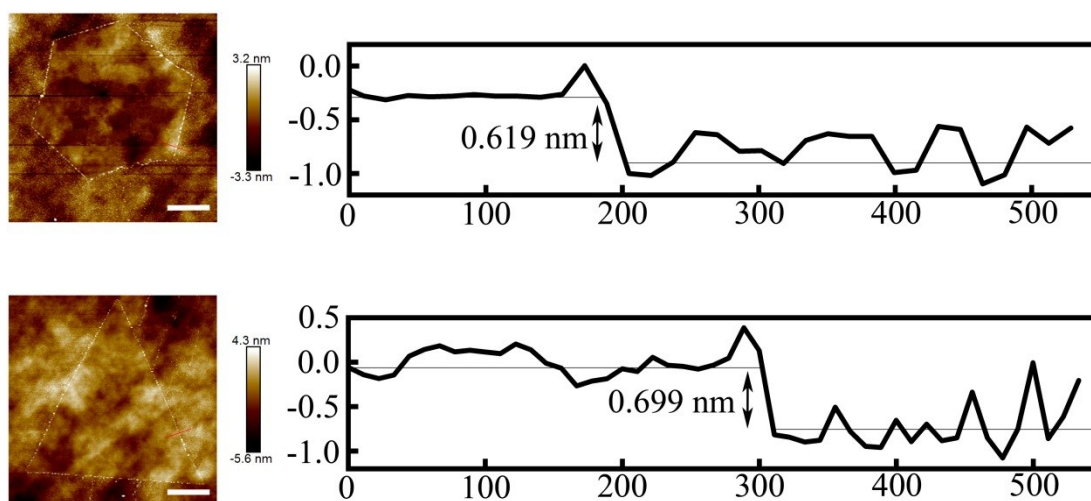


Fig. S5 Atomic force microscopy (AFM) of monolayer (a) hexagonal and (b) triangular flakes.

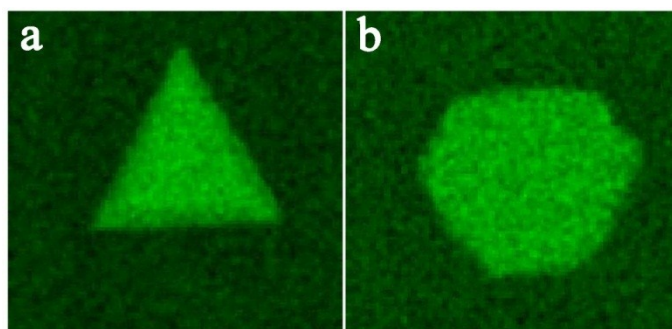


Fig. S6 $A_{1g}(\Gamma)$ Raman mode intensity maps excited in triangle and hexagon MoS_2 domains.



Fig. S7 Transferred monolayer dendritic MoS_2 flakes on glassy carbon.

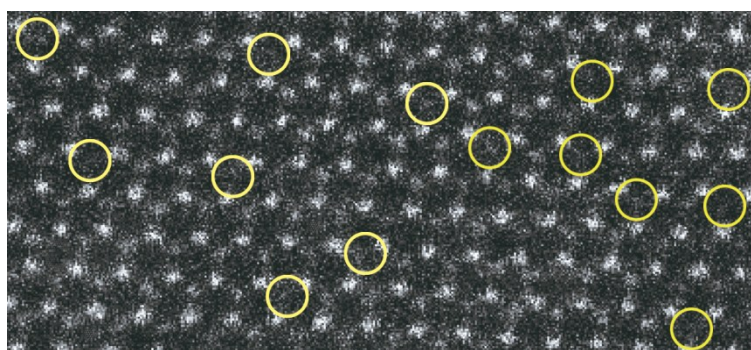


Fig. S8 High-resolution ADF-STEM image of hexagonal flake.

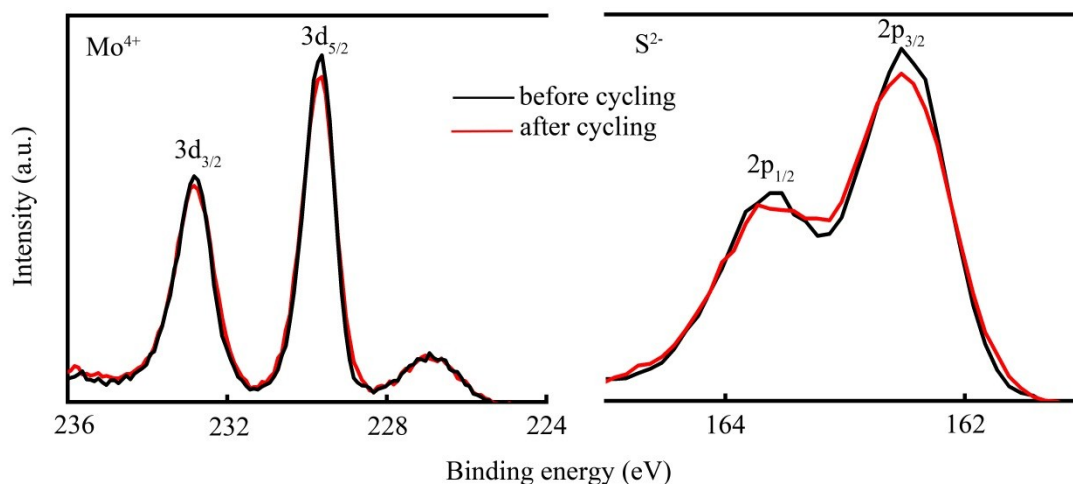


Fig. S9 XPS of monolayer hexagonal flakes before (black curves) and after (red curves) 1000 CV scans.

S1 Electrochemical mechanism

The electrochemical process could be explained according to three principle.[1,2]

In acidic media, three principle steps for converting H^+ to H_2 have been proposed.

Discharge reaction (Volmer):



Electrochemical desorption reaction (Heyrovsky):



Combination reaction (Tafel):



If the reaction (1) accounts for the rate-limiting step, a Tafel slope of ~ 120 mV/dec should result. Tafel slope of 30 or 40 mV/dec is associated with the reaction (2) or (3), which limits the rate after reaction (1).[3,4] The Tafel slope obtained in our work is 53 mV/dec, so the HER process in our work might follow the Volmer-Tafel mechanism. Theoretical and experimental results show that S vacancies act as active sites in HER, where gap states around the Fermi level allow hydrogen to bind directly to the exposed Mo atoms (S vacancies).[5] So on the monolayer basal plane, the intermediate hydrogen adsorbs on the active sites, accepting other intermediate hydrogen to generate H_2 .

A good HER catalyst should form a sufficiently strong bond with adsorbed H^* for facilitation of the proton-couple electron-transfer process, and the bond should also be weak enough to ensure a facile release of gaseous H_2 . [6] Usually, the free energy change for H^* adsorption on a catalyst surface (ΔG_{H^*}) is used to evaluate the adsorption and desorption. According to the calculation result, for intrinsic 2H- MoS_2 ,

the concentrations of S vacancy between 9-19% show the optimum free energy.[5] So, our as-grown defect-rich (with ~13.5% S vacancy concentration) monolayer hexagonal MoS₂ provide an ideal platform to facilitate both H* adsorption and H₂ desorption.

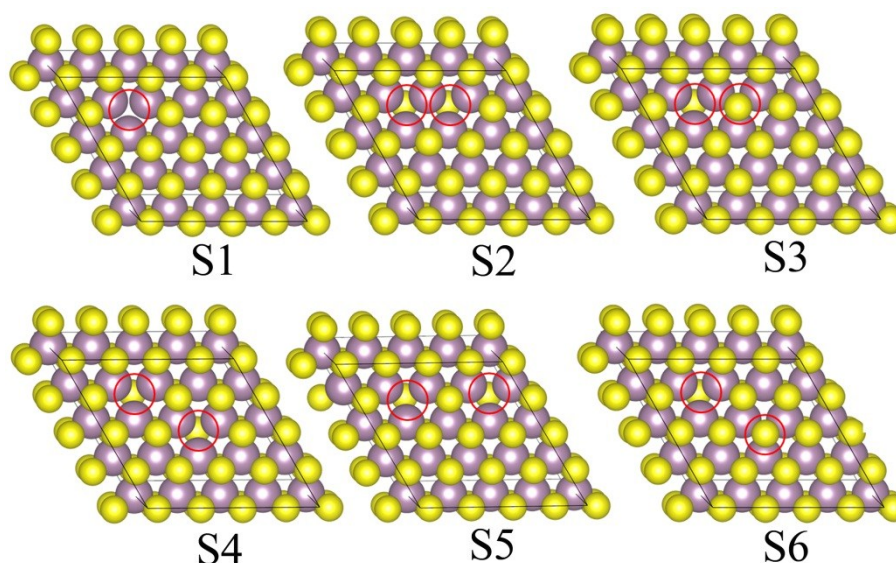


Fig. S10 Possible configurations of two S vacancies appeared in monolayer MoS₂. In S1 configuration, the two S vacancies locate on the opposite side of the basal plane. In S2 to S6 configurations, the two S vacancies locate on the same side of the basal plane

Table S1 Total energy of possible configurations of two S vacancies corresponding to

Fig. S10.

Model	S1	S2	S3	S4	S5	S6
D (Å)	3.12430	3.21134	4.39524	5.52747	6.38063	6.38850
Total energy (eV)	-333.731	-333.732	-333.646	-333.712	-333.657	-333.728

D: distance between two S vacancies.

Because the formation of two S vacancies is random in crystal synthesis, we tested several possible configurations of monolayer MoS₂ in our theoretical calculation models. While fixing the site of one S vacancy, we set up six selectable sites of another S vacancy to calculate the total energies, as shown in table S1. Although the total energies results do not change too much, the most energetically favorable site for the S vacancy is the model S2 in Fig. S10.

References

- [1] S. Shi, D. Gao, B. Xia, P. Liu and D. Xue, *J. Mater. Chem. A*, 2015, **3**, 24414–24421.
- [2] Y. Huang, R. J. Nielsen, W. A. Goddard and M. P. Soriaga, *J. Am. Chem. Soc.*, 2015, **137**, 6692–6698.

- [3] B. E. Conway and B. V. Tilak, *Electrochim. Acta*, 2002, **47**, 3571–3594.
- [4] N. Pentland, J. O. M. Bockris and E. Sheldon, *J. Electrochem. Soc.* 1957, **104**, 182–194.
- [5] H. Li, C. Tsai, A. L. Koh, L. Cai, A. W. Contryman, A. H. Fragapane, J. Zhao, H. S. Han, H. C. Manoharan, F. Abild-Pedersen, J. K. Nørskov and X. Zheng, *Nat. Mater.*, 2016, **15**, 49–53.
- [6] H. Liang, A. N. Gandi, D. H. Anjum, X. Wang, U. Schwingenschlögl and H. N. Alshareef, *Nano Lett.*, 2016, **16**, 7718–7725.